Mutational Spectrum of D-Bifunctional Protein Deficiency and Structure-Based Genotype-Phenotype Analysis

Sacha Ferdinandusse,[1] Mari S. Ylianttila,[2] Jolein Gloerich,[1] M. Kristian Koski,[2] Wendy Oostheim,[1] Hans R. Waterham,[1] J. Kalervo Hiltunen,[2] Ronald J. A. Wanders,[1] and Tuomo Glumoff[2]

[1]Laboratory Genetic Metabolic Diseases, Academic Medical Center at the University of Amsterdam, Amsterdam; and [2]Department of Biochemistry, Biocenter Oulu, University of Oulu, Oulu, Finland

D-bifunctional protein (DBP) deficiency is an autosomal recessive inborn error of peroxisomal fatty acid oxidation. The clinical presentation of DBP deficiency is usually very severe, but a few patients with a relatively mild presentation have been identified. In this article, we report the mutational spectrum of DBP deficiency on the basis of molecular analysis in 110 patients. We identified 61 different mutations by DBP cDNA analysis, 48 of which have not been reported previously. The predicted effects of the different disease-causing amino acid changes on protein structure were determined using the crystal structures of the (3*R*)-hydroxyacyl–coenzyme A (CoA) dehydrogenase unit of rat DBP and the 2-enoyl-CoA hydratase 2 unit and liganded sterol carrier protein 2–like unit of human DBP. The effects ranged from the replacement of catalytic amino acid residues or residues in direct contact with the substrate or cofactor to disturbances of protein folding or dimerization of the subunits. To study whether there is a genotype-phenotype correlation for DBP deficiency, these structure-based analyses were combined with extensive biochemical analyses of patient material (cultured skin fibroblasts and plasma) and available clinical information on the patients. We found that the effect of the mutations identified in patients with a relatively mild clinical and biochemical presentation was less detrimental to the protein structure than the effect of mutations identified in those with a very severe presentation. These results suggest that the amount of residual DBP activity correlates with the severity of the phenotype. From our data, we conclude that, on the basis of the predicted effect of the mutations on protein structure, a genotype-phenotype correlation exists for DBP deficiency.

D-bifunctional protein (DBP) deficiency (MIM #261515) is an autosomal recessive peroxisomal fatty acid oxidation disorder. In the vast majority of cases with DBP deficiency, the clinical presentation is very severe, and most affected children die within the first 2 years of life. Virtually all patients present with neonatal hypotonia and seizures within the 1st mo of life. The majority of patients suffer from visual and hearing impairment and display craniofacial dysmorphic features. Hardly any patients show developmental progress (Wanders et al. 2001). The major metabolic consequences of DBP deficiency are accumulation of (1) very-long-chain fatty acids (VLCFAs), such as C26:0; (2) α-methyl branched-chain fatty acids, like pristanic acid; and (3) the bile acid intermediates di- and trihydroxycholestanoic acids (DHCA/THCA). DBP deficiency can be demonstrated in cultured skin fibroblasts by direct enzyme measurement with the use of trihydroxycholestenoyl–coenzyme A (THC:1-CoA) as substrate and/or by mutation analysis of the gene encoding DBP located on chromosome 5. In addition, deficient β-oxidation activity of C26:0 and pristanic acid—but not of C16:0—measured in cultured skin fibroblasts can be indicative of DBP deficiency. Finally, the presence or absence of the various DBP subunits can be studied by immunoblotting with antibodies against DBP (Wanders et al. 2001).

DBP (also called "multifunctional protein 2," "multifunctional enzyme 2," or "D-peroxisomal bifunctional enzyme") catalyzes the second and third steps of peroxisomal β-oxidation of fatty acids and fatty acid derivatives. It is a homodimeric enzyme with 79-kDa subunits, each of which consists of three functional units: a (3*R*)-hydroxyacyl-CoA dehydrogenase unit, a 2-enoyl-CoA hydratase 2 unit, and a sterol carrier protein 2–like (SCP-2L) unit. DBP is a stereospecific enzyme, since the hydratase unit exclusively forms (*R*)-hydroxyacyl-CoA intermediates from *trans*-2-enoyl-CoAs, which subsequently are oxidized by the dehydrogenase unit into 3-ketoacyl-CoAs (Dieuaide-Noubhani et al. 1997; Jiang et al. 1997*a*; Novikov et al. 1997; Qin et al. 1997). DBP deficiency can be divided into three types, depending on which activity is deficient: (1) type I–deficient patients have a deficiency of both the hydratase and dehydrogenase units of DBP (in fibroblasts of almost all type I–deficient patients, no DBP protein can be detected by immunoblotting with an antibody against human

Received August 3, 2005; accepted for publication October 12, 2005; electronically published November 15, 2005.

Address for correspondence and reprints: Dr. Sacha Ferdinandusse, Laboratory Genetic Metabolic Diseases, Academic Medical Center, F0-224, Meibergdreef 9, 1105 AZ Amsterdam, The Netherlands. E-mail: S.Ferdinandusse@amc.uva.nl

Am. J. Hum. Genet. 2006;78:112–124. 0002-9297/2006/7801-0012$15.00

DBP); (2) type II–deficient patients have an isolated deficiency of the hydratase unit; and (3) type III–deficient patients have an isolated deficiency of the dehydrogenase unit (Wanders et al. 2001). This classification can be made on the basis of enzyme activity measurements in combination with mutation analysis, as described by Gloerich et al. (2003).

DBP is expressed ubiquitously, with the highest mRNA levels in liver (Adamski et al. 1996). In human brain, expression was demonstrated from 13 wk of gestation onward (Itoh et al. 2000). DBP harbors a peroxisomal targeting signal I (C-terminal Ala-Lys-Leu), which ensures peroxisomal localization of the enzyme (Leenders et al. 1994). After import into the peroxisome, the protein is cleaved, resulting in a 35-kDa hydroxyacyl-CoA dehydrogenase unit and a 45-kDa hydratase plus SCP-2L unit (Malila et al. 1993; Jiang et al. 1996, 1997*b*; van Grunsven et al. 1999*b*). The crystal structures of the (3*R*)-hydroxyacyl-CoA dehydrogenase unit of rat DBP and the 2-enoyl-CoA hydratase 2 unit and liganded SCP-2L unit of human DBP have been resolved at high resolution (Haapalainen et al. 2001, 2003; Koski et al. 2005). Like full-length DBP, the recombinant dehydrogenase and hydratase units are both homodimeric, and dimerization appears to be critical for correct folding and enzyme activity. The dehydrogenase unit belongs to the short-chain alcohol dehydrogenase/reductase (SDR) superfamily containing a typical Rossman fold for NAD^+ binding and a Ser-Tyr-Lys triad for catalysis (Filling et al. 2002). It has a two-domain subunit structure, in which the C-terminal domain completes the active site pocket of the neighboring monomer and extends dimeric interactions (Haapalainen et al. 2003). The crystal structure of the hydratase 2 unit revealed a two-domain subunit structure with a complete hot-dog fold (a long α-helix packed against a curved antiparallel β-sheet, which was first described by Leesong et al. [1996]) housing the active site in the C-domain, and, in the N-domain, an incomplete hot-dog fold housing the cavity for the aliphatic acyl part of the substrate molecule (Koski et al. 2005). Although the function of the SCP-2L unit is still unknown, comparison of the crystal structures of unliganded and liganded SCP-2L suggests that a bound substrate analogue leads to structural changes that expose the peroxisomal targeting signal (Haapalainen et al. 2001).

In this article, we report the mutational spectrum for the *DBP* gene in 110 patients who received a clinical and biochemical diagnosis of DBP deficiency. For all disease-causing amino acid changes, the effect on the protein structure was analyzed by introducing the amino acid changes *in silico* in models of the crystal structures of the functional domains of DBP. To study whether there is a genotype-phenotype correlation, these structure-based analyses were combined with extensive biochemical analyses of patient material (cultured skin fibroblasts and plasma) and available clinical information on the patients.

Subjects and Methods

Patients

After informed consent was obtained, skin fibroblasts from all patients included in this study were sent to the Laboratory Genetic Metabolic Diseases for diagnostic purposes. DBP deficiency was determined by direct enzyme activity measurements in cultured skin fibroblasts, with the use of THC:1-CoA as substrate (van Grunsven et al. 1998), and was substantiated by the following biochemical analyses: (1) α-oxidation of phytanic acid (Wanders and Van Roermund 1993), (2) β-oxidation of C26:0, pristanic acid, and C16:0 (Wanders et al. 1995), (3) analysis of VLCFA levels (Vreken et al. 1998), (4) immunoblot analysis of DBP, and (5) catalase and DBP immunofluorescence (van Grunsven et al. 1999*b*). When plasma was available, the levels of VLCFAs, phytanic acid, pristanic acid, and bile acids were measured (Vreken et al. 1998; Bootsma et al. 1999).

Mutation Analysis

DBP mutation analysis was performed by sequencing of DBP cDNA. Total RNA was isolated from primary skin fibroblasts by use of the TRIzol reagent (Invitrogen). The coding region was amplified by PCR in three overlapping fragments from first-strand cDNA prepared from total RNA, as described elsewhere (van Grunsven et al. 1998). Forward and reverse primers used for mutation analysis were tagged with a −21M13 sequence and an M13rev sequence, respectively. PCR fragments were sequenced in two directions by use of the "−21M13" and "M13rev" fluorescent primers on an Applied Biosystems automated DNA sequencer, in accordance with the manufacturer's protocol (Applied Biosystems).

Homozygosity for the c.46G→A (G16S) and c.1369A→T (N457Y) mutations was checked at the genomic level by restriction analysis. DNA was isolated from skin fibroblasts by use of the Wizard Genomic DNA purification kit (Promega). PCR was performed with primers 5′-ACTACATTTCCCA-3′ and 5′-TTCGCATGCTCACCTGCCCC-3′ for the c.46G→A mutation and with primers 5′-ACTGGCCAATAAC-3′ and 5′-CACTGGCAGTCATA-3′ for the c.1369A→T mutation. Subsequently, restriction analysis was performed with *Msp*I (Roche), which only cuts when the c.46G→A mutation is not present, and with *Bsr*I (New England Biolabs), which does not cut when the c.1369A→T mutation is present.

Structure Analysis

The crystal structures of the functional domains of DBP used for analysis, which have been reported elsewhere, are rat (3*R*)-hydroxyacyl-CoA dehydrogenase (Haapalainen et al. 2003), human 2-enoyl-CoA hydratase 2 (Koski et al. 2005), and human SCP-2L domain (Haapalainen et al. 2001), corresponding to entries 1GZ6, 1S9C, and 1IKT, respectively, of the Protein Data Bank (PDB) (Berman et al. 2000). Amino acid residues affected by the disease-causing mutations were spatially lo-

Table 1

Mutations Identified in 110 Patients with DBP Deficiency Identified by DBP cDNA Sequencing

Nucleotide Change[a]	Exon	Predicted Effect on Coding Sequence[b]	No. of Patients Identified[c]		Allele Frequency	DBP Type	Reference[d]
			Homozygous	Heterozygous			
Missense:							
c.43A→G	1	T15A	1	…	.9	III	
c.46G→A	1	G16S	25	3	24.1	III	van Grunsven et al. 1998
c.50C→T	1	A17V	1	…	.9	III	
c.63G→T	2	L21F	1	…	.9	III	van Grunsven et al. 1999*b*
c.76G→C	2	A26P	1	…	.9	III	
c.101C→T	2	A34V	…	1	.5	III	
c.216C→A	3	N72K	1	…	.9	III	
c.311G→T	6	R104M	1	…	.9	III	
c.377G→T	7	G126V	1	…	.9	III	
c.394C→T	7	R132W	1	…	.9	III	
c.458C→T	8	S153L	1	…	.9	III	
c.472A→G	8	N158D	…	1	.5	III	
c.485C→A	8	A162D	1	…	.9	III	
c.530C→T	8	S177F	1	…	.9	III	Paton and Pollard 2000
c.652G→T	9	V218L	2	1	2.3	III	Paton and Pollard 2000
c.694G→A	9	E232K	1	…	.9	III	
c.710T→C	9	F237S	…	1	.5	III	
c.721G→A	10	A241T	1	…	.9	III	
c.725G→A	10	G242E	1	…	.9	III	
c.742C→T	11	R248C	3	1	3.2	III	
c.745T→G	11	W249G	…	1	.5	III	
c.819G→T	11	W273C	2	1	2.3	III	
c.1042G→A	13	A348T	…	1	.5	II	
c.1097A→G	13	E366G	1	…	.9	II	
c.1214T→C	14	L405P	1	…	.9	II	
c.1369A→T	16	N457Y	11	2	10.9	II	van Grunsven et al. 1999*a*
c.1369A→G	16	N457D	…	1	.5	II	Paton and Pollard 2000
c.1516C→T	18	R506C	3	…	2.7	II	
c.1517G→A	18	R506H	1	…	.9	II	
c.1528G→T	18	D510Y	1	…	.9	II	
c.1547T→C	18	I516T	…	2	.9	II	
c.1586C→T	19	P529L	1	…	.9	II	
c.1595A→G	19	H532R	1	…	.9	II	
c.1597G→C	19	G533R	1	…	.9	II	
Nonsense:							
c.672G→A	9	W224X	1	…	.9	I	
c.2029G→T	23	Q677X	1	…	.9	I	
Deletion:							
c.45delC	1	G16fsX19	…	1	.5	I	
c.113_220del	3	V38_Y73del	1	1	1.4	I	Ferdinandusse et al. 2002
c.130delG	3	D44fsX10	…	1	.5	I	
c.221_280del	4	S74_D94del	…	1	.5	I	
c.233_235del	4	R65del	…	1	.5	III	
c.230_289del	4–5	E77_V97del	…	1	.5	…	
c.281_302del	5	D94fsX3	3	…	2.7	I	
c.281_622del	5–8	D94_E207del	5	…	4.5	I	van Grunsven et al. 1999*b*
c.303_349del	6	I102fsX48	1	…	.9	I	Paton and Pollard 2000
c.422_423del	7	K142fsX23	1	…	.9	I	van Grunsven et al. 1999*b*
c.435_622del	8	I146fsX23	…	1	.5	I	
c.623_714del	9	D208fsX29	1	…	.9	I	
c.715_1261del	10–14	V239fsX3	1	…	.9	I	
c.740_868del	11	L740X	1	…	.9	I	
c.788delC	11	P263fsX2	1	…	.9	I	
c.824_826del	11	K275del	…	1	.5	III	
c.869_881del	12	E290fsX2	5	…	4.5	I	van Grunsven et al. 1999*b*
c.1210_1261del	14	V404fsX3	2	…	1.8	I	Suzuki et al. 1997
c.1210_1333del	14–15	V404fsX36	1	…	.9	I	
c.1262_1333del	15	G421_D444del	1	…	.9	II	
c.1438_1503del	17	V480_Q501del	1	…	.9	II	van Grunsven et al. 1999*b*
c.1936_1993del	22	V646fsX4	1	…	.9	I	

(*continued*)

Table 1 (continued)

Nucleotide Change[a]	Exon	Predicted Effect on Coding Sequence[b]	No. of Patients Identified[c]		Allele Frequency	DBP Type	Reference[d]
			Homozygous	Heterozygous			
Insertion:							
c.112_113ins 65 nt	3	V38fsX23	1	1	1.4	I	
c.941_942insG	12	S314fsX53	…	1	.5	I	
c.972_973insTGTTCTTAG	13	A325fsX3	1	…	.9	I	

Note.—Combination of alleles were as follows. Type II deficiency: N457Y+I516T (1 patient), N457D+I516T (1), N457Y+45delC (1), and A348T+221_280del (1); type III deficiency: G16S+N158D (1), G16S+230-289del (1), A34V+F237S (1), delR65+delK275 (1), V218L+W237S (1), and R248C+W249G (1).

[a] The numbering of nucleotides starts at the first adenine of the translation initiation codon.

[b] The numbering of amino acids starts at the first methionine encoded by the translation initiation codon.

[c] Homozygosity and heterozygosity refer to the appearance of mutations at the cDNA level.

[d] All mutations with no indicated reference are novel.

cated, and their effect on the protein structure was analyzed. Atomic models of the structures were visualized from structural coordinates by use of the programs O (Jones et al. 1991) and Swiss-PDBViewer (Guex and Peitsch 1997) on a computer graphics workstation, which allowed both the measurement of any relevant interatomic distances and the introduction of the amino acid changes *in silico*. When appropriate, structure and sequence homologies to corresponding proteins from other species were used as reference—namely, the amino acid sequence of human (3*R*)-hydroxyacyl-CoA dehydrogenase (Adamski et al. 1995) and the crystal structures of yeast *Candida tropicalis* (3*R*)-hydroxyacyl-CoA dehydrogenase dimer (M. S. Ylianttila, N. Pursiainen, A. Juffer, Y. Poirier, J. K. Hiltunen, and T. Glumoff, unpublished data) and liganded 2-enoyl-CoA hydratase 2 (Koski et al. 2004). After the experimental work was completed, the crystal structure of the human (3*R*)-hydroxyacyl-CoA dehydrogenase became available (PDB entry 1ZBQ). The rat and human dehydrogenase sequences are 87.4% identical and 93.8% similar to each other. All the amino acids, except S177, that are mutated in DBP type III–deficient patients described in this work are conserved in rat and human.

Results

Mutation Analysis

Sequence analysis of the *DBP* cDNA of 110 patients (excluding sibs) who received a clinical and biochemical diagnosis of DBP deficiency revealed 61 different mutations, 48 of which have not been reported previously. The mutations are detailed in table 1 and include 22 deletions, 3 insertions, 2 nonsense mutations, and 34 missense mutations. It should be noted that 13 of the 22 deletions comprise the skipping of one or more exons and therefore are most likely due to splice-site mutation. The location of all missense mutations is indicated in the amino acid sequence of DBP that has been supplemented with secondary structural elements in figure 1. If we assume that all apparent homozygotes at the cDNA level are true homozygotes, the missense mutation G16S is by far the most common mutation causing DBP deficiency (type III), which had an allele frequency of ~24% and was detected in 28 of the 110 patients. For four of the seven apparent-homozygous patients, homozygosity was confirmed at the genomic level. The second most common mutation causing DBP deficiency (type II) is the missense mutation N457Y, which had an allele frequency of ~11% and was found in 13 patients. Of five patients for whom homozygosity was checked, two turned out to be heterozygotes at the genomic level. Other relatively common mutations were c.281_622del and c.869_881del (each identified in five patients; allele frequency ~4.5%) and R248C (four patients; allele frequency ~3.2%). All other mutations were identified in only one, two, or three patients.

In DBP type I–deficient patients, only deletions, insertions, and nonsense mutations were identified (table 1). All deletions resulted in a truncated protein, except for three large in-frame deletions. Interestingly, in two type I–deficient patients, the truncation of DBP occurred only in the C-terminal SCP-2L unit. No protein (neither the full-length 79-kDa protein nor the 45-kDa hydratase or 35-kDa dehydrogenase unit) was detected by immunoblotting in fibroblast homogenates from these patients. No formation of 24-OH-THC-CoA from THC: 1-CoA could be measured in fibroblasts, and further studies of the Q677X mutation revealed that, in addition, no dehydrogenase activity could be measured when it was assayed independent of the hydratase activity (Gloerich et al. 2003).

Two patients with DBP type II deficiency had in-frame deletions in the hydratase unit, one with a deletion of 22 aa and the other with a deletion of 24 aa. Immunoblotting experiments revealed the absence of the 45-kDa hydratase unit, but the 35-kDa dehydrogenase unit was present, although it was lower in abundance than in control fibroblasts. In addition, DBP dehydrogenase

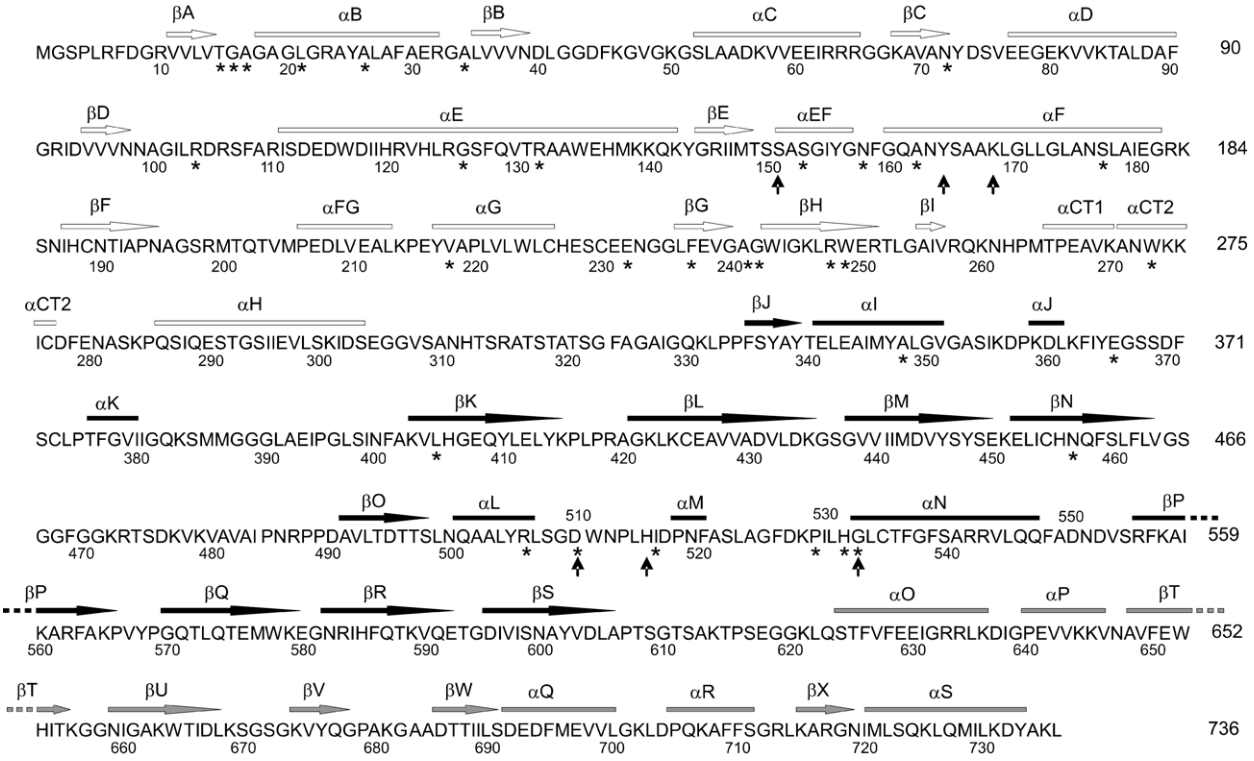

Figure 1 Amino acid sequence of human DBP. Secondary structural elements are indicated above the sequence as either bars (α-helices) or arrows (β-strands) (a continuation to the following line is shown as three dots). Names of the helices and strands are indicated above the symbols. αCT1 and αCT2 are the COOH-terminal α-helices of the (3*R*)-hydroxyacyl-CoA dehydrogenase unit. Shading indicates the functional units: (3*R*)-hydroxyacyl-CoA dehydrogenase (*white*), 2-enoyl-CoA hydratase 2 (*black*), and sterol carrier protein 2–like (*gray*). The identified missense mutations within our cohort of DBP-deficient patients are marked with an asterisk (*). Catalytic residues of the two enzymatic units are marked with vertical arrows.

activity could be measured, whereas DBP hydratase activity was deficient (Gloerich et al. 2003). All other DBP type II–deficient patients had missense mutations in the coding region of the DBP hydratase unit.

DBP type III deficiency was predominantly caused by missense mutations and, in two cases, by a 1-aa deletion in the coding region of the dehydrogenase unit. One type III–deficient patient had the most common missense mutation, G16S, on one allele and had an in-frame deletion of 20 aa (E77_V97del) on the other allele. Fibroblasts from this patient displayed abundant DBP hydratase activity, justifying classification as type III deficiency.

Structure Analysis

With the help of the crystal structures that have been determined for all three DBP units, the mutations identified in our cohort were located spatially, and their effect on protein structure was analyzed *in silico*. The structural changes caused by the different disease-causing mutations ranged from a replacement of a single amino acid residue, resulting in the loss of a crucial bond with nearby amino acid residues, to proteins with deletions in the polypeptide chain, or truncated proteins. On the basis of our analysis, we grouped the mutations in accordance with their assumed structural disturbances. These categories are presented in table 2 and will be discussed below. For some mutations, the current structural knowledge about DBP is not sufficient to explain the enzyme dysfunction. These mutations are grouped under the category "Others" in table 2.

Investigation of the mutations in DBP type I–deficient patients revealed that they all result in structural anomalies affecting the DBP protein as a whole. The majority of patients had a deletion or an insertion at the cDNA level that caused a frameshift and resulted in a prematurely terminated polypeptide chain. In two patients, the DBP protein was truncated because of a nonsense mutation, whereas the others had large in-frame deletions. Interestingly, the two mutations that cause a truncation in the C-terminal SCP-2L unit (Q677X and c.1936_1993del) suggest that an intact SCP-2L domain might be necessary for correct folding of the full-length DBP. However, since there is no experimental structural model of the assembly of the domains into a functional

Table 2

Mutations That Cause DBP Deficiency Types II and III, Grouped by Mechanism of Structural Disturbance

DBP Deficiency and Disturbance Mechanism	Mutation(s)
Type II deficiency (hydratase unit):	
Disturbance of:	
Ligand interaction	G533R, L405P
Active site architecture	D510Y, P529L, H532R
Dimerization	E366G, R506C, R506H, I516T
Domain folding	N457Y, G421_D444del, V480_Q501del
Others[a]	A348T, N457D
Type III deficiency (dehydrogenase unit):	
Disturbance of:	
Ligand interaction	N158D
Nucleotide binding	T15A, G16S, A17V, L21F, A26P, N72K, G126V, V218L
Active site architecture	S153L
Dimerization of:	
Two nucleotide-binding domains	R132W, A162D, S177F
Nucleotide-binding domain and C-domain	E232K, F237S, A241T, G242E, W273C
Two C-domains	R248C, W249G
Domain folding	del K275
Others[a]	A34V, del R65, R104M

[a] The category "Others" includes mutations for which the reason for the structural disturbance is not obvious in light of the current structural knowledge of DBP.

DBP, the structural basis of these disease-causing variants remains unknown. It is also possible that these proteins are enzymatically active but are not transported to peroxisomes, since the truncation removes the peroxisomal targeting signal.

In cases of DBP type II or type III deficiency, the fatal disturbance of the overall structure of the DBP protein and its enzyme activity was often caused by a seemingly small defect. The amino acid changes found in type II– or type III–deficient patients resulted in replacement of catalytic residues or residues in direct contact with the substrate or cofactor or resulted in disturbed protein folding or dimerization of the subunits (see table 2). Obviously, if a residue crucial for enzymatic function is replaced, like the catalytic D510 of the hydratase 2 unit in one patient, activity is lost. When the mutation replaces a residue in contact with the substrate with a residue incapable of forming that contact, the enzymatic activity is also lost. For example, L405 is located at the entrance of the substrate-binding tunnel of the hydratase 2 unit. The change of this leucine to a proline, a mutation identified in one patient, could alter the bending of the β-strand βK—as predicted by our modeling studies—thereby breaking hydrophobic interactions with the panthetheine moiety of the CoA-ester and thus rendering substrate binding unfavorable. Enzyme activity is also lost if the nucleotide-binding domain of DBP cannot bind the cofactor NAD^+. The most common mutation, G16S, is an example of such a disturbance. Glycine 16 sits in, and actually shapes, a short loop (fig. 2*A4*) that provides space for the adenine ring of NAD^+. Any other side chain in this position reshapes the loop and prevents NAD^+ binding, because of a steric clash.

Fourteen different mutations were identified that affect dimerization of DBP (table 2). DBP dimerization is achieved through specific contacts between its enzymatic units, which have been resolved from crystal structures. These contacts are straightforward between two hydratase 2 monomers, since they consist of pairing via relatively flat surfaces (fig. 2*B*), whereas the dimerization between two dehydrogenase monomers is more complex. Each dehydrogenase monomer consists of a nucleotide-binding domain and a C-terminal domain that stretches out from the folded monomer. Two monomers form an intertwined dimer, where the C-terminal domain comes in close contact with the nucleotide-binding domain of the neighboring monomer (fig. 2*A*). This results in three kinds of dimerization contacts: (1) between two nucleotide-binding domains, (2) between two C-terminal domains, and (3) between a nucleotide-binding domain and a C-terminal domain. Alterations in any of the dimerization contacts may lower the enzyme activity, because of protein instability, or render it inactive. Interestingly, four mutations in our cohort (I516T, A241T, W273C, and R248C) located at the dimerization interface of the subunits do not abolish dimerization completely, as predicted by our modeling studies, probably because dimerization is achieved via a network of contacts and none of the affected residues is solely responsible for dimerization (table 2 and fig. 2).

Even when contacts between different domains or between the protein and substrate/cofactor are not dis-

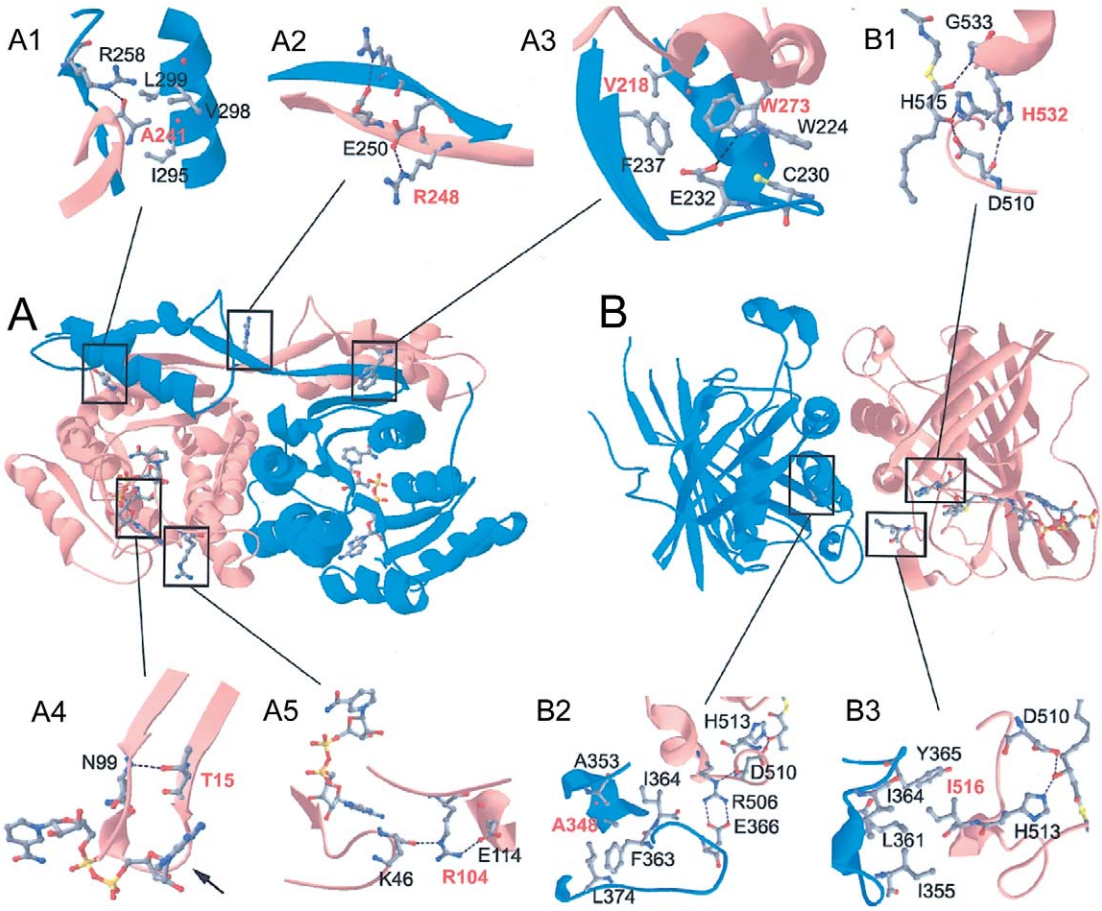

Figure 2 The three-dimensional dimeric structures of the enzymatic units of DBP. *A,* Ribbon representation of the dehydrogenase unit of rat DBP (PDB entry 1GZ6). The two monomers are colored red and blue. The stick representations of the two NAD^+ molecules and the amino acid residues are colored as follows: carbon, gray; oxygen, red; nitrogen, blue; phosphorus, yellow. The boxes indicate parts of the structure that are shown in greater detail in panels A1–A5, which show the amino acid residues (*red*) that are mutated in DBP type III–deficient patients with a mild clinical presentation (see main text for details). The black arrow in panel A4 indicates the conserved loop of SDR enzymes important in NAD^+ binding and that contains the G16 residue. The G16S change is the most common mutation causing DBP deficiency. *B,* Ribbon representation of the hydratase 2 unit of human DBP (PDB entry 1S9C). The reaction product, (3*R*)-hydroxydecanoyl-CoA, has been docked to the right subunit by use of the structure of the yeast *C. tropicalis* ortholog (PDB entry 1PN4) as a model. The colors are the same as in panel A, with the addition of the sulphur atom in the CoA molecule (*bright yellow*). Panels B1–B3 show the amino acids (*red*) that are mutated in DBP type II–deficient patients with a mild clinical presentation. In panel B1, the interaction between the substrate molecule and the catalytic residues is shown together with the formed oxyanion hole between G533 and the carboxyl group of the substrate. In panel B2, the mutation site A348 is shown together with the salt bridge between E366 and R506, since both these residues are also mutated within our cohort.

turbed, a change in amino acid residue can affect folding of the DBP polypeptide locally. This can occur, for example, when the side chain of the replacement amino acid does not fit into the available space, or when a polar side chain is introduced into a hydrophobic pocket. These changes can lead to multiplicative rearrangements in the structure, which ultimately results in a nonfunctional enzyme. The mutation I516T, in addition to being involved in dimerization contacts, introduces a hydrophilic residue into a hydrophobic environment right next to the active site H515 in the structurally conserved hydratase 2 motif and breaks the active site conformation (fig. 2*B3*). A change into another hydrophobic residue would probably be tolerated in this position, since some eukaryotes have a leucine or a valine instead of an isoleucine at position 516 (Qin et al. 2000).

Structure-Based Genotype-Phenotype Analysis

Virtually all patients who have DBP deficiency display a severe clinical phenotype and die early in life. Patients with deletions, insertions, and nonsense mutations leading to a truncated enzyme never survive >1 year. However, most patients with missense mutations also die in

the first 2 years of life. The age at death of patients who are apparent homozygous for the most common mutations in the hydratase domain (N457Y) and in the dehydrogenase domain (G16S) ranged from 1 to 26 mo and from 1 to 24 mo, respectively.

Of 78 patients for whom information about survival was available, only 8 (including 2 sib pairs) survived >36 mo. These patients had missense mutations in the coding region for either the hydratase 2 unit (three patients) or the dehydrogenase unit (five patients). In most cases, the mutations associated with a mild phenotype resulted in amino acid changes that affected dimerization or minor structural alternations, rather than resulting in a direct impact on nucleotide or substrate binding. The mutations observed to cause a mild clinical and biochemical presentation (see table 3) are discussed below in view of the structural details, and a genotype-phenotype analysis is presented.

One of two sisters with DBP deficiency died at age 43 mo (the other sister's age at death is unknown) and was an apparent homozygote for the H532R mutation. Only the 35-kDa dehydrogenase band was visible on Western blot. Pristanic acid and C26:0 β-oxidation activities were very low: 16 pmol/h/mg and 96 pmol/h/mg, respectively (control range 691–2,178 pmol/h/mg for pristanic acid and 1,025–2,994 pmol/h/mg for C26:0 β-oxidation), and C26:0 accumulation in fibroblasts was substantial at 1.38 μmol/g (control range 0.18–0.38 μmol/g). The bile acid intermediates DHCA and THCA were detectable in plasma. The H532R mutation is one of very few mutations for which, perhaps somewhat surprisingly, a survival of >36 mo was observed despite the fact that the mutation disturbs the active site architecture. The histidine at position 532 in the hydratase 2 unit is highly conserved in eukaryotic DBPs. A change to arginine causes a disturbance at the active site because of the bulkier size of the arginine side chain. This is supported by experiments with the yeast enzyme, in which a mutation to alanine does not abolish the enzyme activity (Qin et al. 2000). The stabilizing stacking interaction of the imidazole ring of H532 with the corresponding side chain of the catalytic H515 can no longer take place (fig. 2*B1*). Interestingly, a mutation at the neighboring residue, G533R, resulted in a more severe clinical presentation owing to the fact that this glycine is implicated in the formation of the oxyanion hole needed for stabilizing the reaction intermediate. The bulkier arginine will be hindered sterically in positioning its backbone amide similarly as glycine.

A boy with consanguineous parents had a homozygous A241T change and survived to age 48 mo (Schröder et al. 2004). Western blotting revealed DBP protein; however, the abundance of the dehydrogenase unit was lower than in control fibroblasts. Although β-oxidation activity for pristanic acid was low (11 pmol/h/mg), there was considerable residual activity with C26:0 (461 pmol/h/mg) as substrate. Strikingly, VLCFAs and phytanic acid did not accumulate in plasma of this patient. The A241T change breaks a Van der Waals interaction between Cβ of A241 (in the nucleotide-binding domain of one dehydrogenase monomer) and either Cγ1 of V298 or Cδ1 of L299 (in the C-terminal domain of the other monomer). In addition, the threonine side chain is polar and does not fit perfectly into the space available for alanine (fig. 2*A1*). It is noteworthy that this mutation appears to not disrupt the hydrogen bond between main-chain carbonyl oxygen of residue 241 and NH1 of arginine 258, thus tempering the disturbing effect of the mutation. A nearby mutation, G242E, disturbs the protein structure more, because of the collision

Table 3

Mutations and Biochemical Analyses Performed in Skin Fibroblasts and Plasma of DBP-Deficient Patients with a Prolonged Survival

			Cultured Skin Fibroblasts			Plasma Levels (μmol/liter)			
Subject(s)	Genotype at cDNA Level	Survival	C26:0 Level (μmol/g)	C26:0 β-Oxidation (pmol/h/mg)	Pristanic Acid β-Oxidation (pmol/h/mg)	C26:0	THCA	Phytanic Acid	Pristanic Acid
Controls[a]	…	…	.29 ± .12	1,438 ± 484	1,402 ± 533	.74 ± .26	0 ± 0	2.4 ± 3.0	.2 ± .3
Patient 1	H532R	43 mo (D)	1.38	96	16	↑	↑	ND	ND
Patient 2	A241T	48 mo (D)	.59	461	11	N	ND	N	N
Patient 3	R248C[b]	>5 years	2.04	243	28	↑	N	N	N
Patient 4	A348T/c.221_280del	>7.5 years	.75	595	16	ND	ND	ND	ND
Patient 5	T15A	>8 years	.56	1,302	108	N	N	N	N
Patient 6	R104M	>8.5 years	.43	590	40	N	N	N	N
Patient 7	V218L/W273C	>12 years	.13	501	106	↑	N	N	N
Patient 8	N457D/I516T	>13.5 years	.56	578	30	ND	ND	ND	ND

Note.—Upward-pointing arrow (↑) = increased; (D) = deceased; N = within control range; ND = not determined.

[a] Values for controls are given as median ± interquartile range.

[b] Patient 3 is heterozygous for this mutation at the genomic level.

between the C-terminal domain of one dehydrogenase subunit and the nucleotide-binding domain of the other dehydrogenase subunit in the dimer, resulting in a more severe biochemical and clinical presentation in the patient.

A girl, who was >5 years old at the latest follow-up, was homozygous for the R248C mutation at the cDNA level but heterozygous at the genomic level. The biochemical phenotype was relatively mild in this patient, with no accumulation of DHCA/THCA and normal levels of phytanic and pristanic acids, and, although C26:0 levels were elevated in plasma, the ratio C26/C22 was near normal. Structure analysis supports the mild phenotype. The β-sheets H from both dehydrogenase monomers intersect and form salt bridges between NH1 of R248 and Oε2 of E250. Although these contacts are broken by the R248C mutation (fig. 2*A2*), other contacts involved in dimerization probably cause enough cohesiveness for residual DBP activity. On the basis of a hypothetical but well-justified model of the assembly of the units into a mature DBP (Koski et al. 2005), it can be predicted that this region is also in contact with the hydratase unit, thus buffering the effects caused by mutations in this region of DBP.

At first, only one heterozygous mutation (A348T) could be found at the cDNA level in a girl who was still alive at age 7.5 years. Further detailed analysis revealed a heterozygous deletion of exon 4 (c.221_280del), most likely caused by missplicing, leading to an in-frame deletion of 20 aa. Strikingly, predominantly normally spliced mRNA was present, indicating that the missplicing does not always occur. This probably causes the mild clinical and biochemical presentation in the patient. A348T is, from a structural point of view, an intriguing mutation because a contact to a surface loop structure is affected. Because of their mobility, loops frequently make the outcome of structure analysis uncertain. Alanine 348, located in the first α-helix of the hydratase unit, contributes hydrophobic interactions to the N-terminal overhanging loop structure (fig. 2*B2*). This loop contains a glutamate (position 366), which is important for dimerization (Koski et al. 2005). Therefore, introduction of a polar threonine may result in local reorganization of the overhanging loop and may affect dimerization.

The only patient with normal C26:0 β-oxidation activity in fibroblasts was a girl with consanguineous parents and a homozygous T15A mutation. At her latest follow-up, she was >8 years old, but her condition was progressively deteriorating. In contrast to C26:0 oxidation, pristanic acid β-oxidation was deficient, and VLCFA levels were increased in fibroblasts. Catalase immunofluorescence revealed normal appearance of peroxisomes in number and punctation, and investigations in plasma revealed no abnormalities. T15 forms a hydrogen bond with the main chain nitrogen of N99, a common structural feature among the SDR family (Filling et al. 2002), and this interaction holds together two β-strands immediately below the NAD^+ binding site (fig. 2*A4*). A15 cannot form this hydrogen bond and thus potentially loosens the cofactor-binding groove. However, this effect is less detrimental than the effect of the common G16S mutation.

A girl with consanguineous parents and a homozygous R104M mutation at the cDNA level was age 8.5 years at the latest follow-up. After she had reached some developmental milestones (she was able to sit and stand unsupported for 5 s and had voluntary control of hand function), her condition progressively deteriorated. The diagnosis of DBP deficiency was missed at first because VLCFA, pristanic acid, phytanic acid, and bile acid levels were normal in plasma. Subsequent studies in fibroblasts revealed abnormalities, although there was a substantial residual C26:0 β-oxidation activity (590 pmol/h/mg). This mutation is another example (besides A348T) in which stabilization of a surface loop structure in the protein seems to be disturbed. R104 sits in a loop that is close to another loop just above the nucleotide-binding groove (fig. 2*A5*). The loop is implicated in substrate binding, since it is missing from monomer B of *C. tropicalis* (3*R*)-hydroxyacyl-CoA dehydrogenase, which is active only with short-chain fatty acyl-CoAs, whereas monomer A, which does contain the loop, shows activity with medium- and long-chain fatty acyl-CoAs (Qin et al. 1999).

Two siblings were compound heterozygous for V218L and W273C. The girl died at age 10 years and 7 mo, whereas the boy was still alive at age 12 years and 2 mo. Studies of fibroblasts from the boy revealed that DBP protein was present normally on western blot, that catalase immunofluorescence and VLCFAs were normal, and that β-oxidation activity was 501 pmol/h/mg for C26:0 and 106 pmol/h/mg for pristanic acid. In plasma, VLCFA levels were only slightly abnormal, whereas no abnormalities were found for the bile acids, pristanic acid, and phytanic acid. In our cohort, two other patients were homozygous for the V218L mutation at the cDNA level, and two patients were homozygous for the W273C mutation. At the biochemical level, the phenotype of these four patients was much more severe than that of the siblings, and one boy with the W273C mutation died at age 3 mo. Structurally, W273C breaks dimerization contacts between the nucleotide-binding domain and the C-terminal domain of the neighboring subunit in the dehydrogenase dimer in two ways: a hydrogen bond between Nε1 of the tryptophan and Oε1 of E232 can no longer be formed and also the Van der Waals interactions of W273 (Cζ2 and CH2) with aromatic side chains of F237 (Cζ) and W224 (Cδ1) cannot be formed (fig. 2*A3*). Introduction of a leucine instead of the

smaller valine at position 218 in the α-helix G, on the other hand, pushes the helix outward because of a steric clash. The combination of the two mutations—V218L affecting nucleotide-binding and W273C affecting dimerization—probably causes the mild phenotype in the two siblings by a fortuitous structural countereffect of the mutations.

The oldest patient in our cohort was age 13.5 years at the latest follow-up and was a compound heterozygote for N457D and I516T. A patient with the mutation combination N457Y and I516T died at age 11 mo, which indicates that the N457D mutation causes a much milder phenotype than does the common N457Y change. Elsewhere, this mutation was described in a patient >16.5 years old (Paton et al. 1996, 2002). However, the described patient was heterozygous for this mutation, and, although the other allele seemed to be expressed only in low amounts, no other mutation was found, which prevented any conclusion from being drawn from this case about genotype-phenotype correlation. A possible structural explanation for why the N457D mutation is milder than the N457Y mutation is that, whereas the bulky tyrosine side chain does not fit into the space available for the asparagine, aspartate is the same size as asparagine. In addition, an aspartate can restore a hydrogen bond (Koski et al. 2005)—in this case, between a terminal carbonyl oxygen from D457 and a backbone nitrogen of G378—in contrast to tyrosine.

To investigate the N457D mutation further, we studied possible temperature sensitivity by culturing the fibroblasts from our type II–deficient patient, a control subject, and two type I–deficient patients (one with c.715_1261del and one with the nonsense mutation Q677X) at 30°C, 37°C, and 40°C for 7 d. We then measured DBP activity, determined VLCFA levels, measured rates of β-oxidation with different substrates, and performed immunofluorescence and immunoblot analyses. For all patients, the in vitro DBP dehydrogenase activity was absent at all temperatures (not shown), but, strikingly, C26:0 β-oxidation became completely normal at 30°C, and pristanic acid oxidation increased considerably in the patient with the N457D mutation (see table 4). In addition, VLCFA levels were near normal at 30°C and 37°C for this patient but became strongly elevated at 40°C, to a similar extent as for the type I–deficient patients. Immunoblotting revealed the complete absence of DBP protein in fibroblasts of the type I–deficient patients at all temperatures, whereas the full-length protein and the 35-kDa band were present at 30°C and 37°C in the type II–deficient patient with a mild phenotype (see fig. 3*A*). At 40°C, the abundance of the full-length protein decreased considerably, and the 35-kDa band disappeared completely. Furthermore, immunofluorescence with an antibody against DBP was normal at 30°C and 37°C in the patient with the N457D mutation, but, at 40°C, staining of peroxisomes was absent, just like in the fibroblasts from the type I–deficient patients at all temperatures (fig. 3*B*).

Concluding Remarks

In this article, we report the results of mutation analyses in a large cohort of DBP-deficient patients. The effects

Table 4

Fatty Acid Oxidation Measurement and VLCFA Analysis in Fibroblasts of a Control Subject and of DBP-Deficient Patients Cultured at 30°C, 37°C, and 40°C

	Fatty Acid Oxidation			VLCFA Analysis		
Culture Temperature and Sample	C26:0 (pmol/h/mg)	Pristanic Acid (pmol/h/mg)	Phytanic Acid (pmol/h/mg)	C26:0 (μmol/g)	C24/C22 (ratio)	C26/C22 (ratio)
30°C:						
Control	1,245	1,084	43	.25	1.99	.05
DBP deficiency:						
Type I (c.715_1261del)	229	16	8	1.84	2.07	.41
Type I (Q677X)	…	…	…	2.21	2.22	.44
Type II (N457D+I516T)	1,109	199	39	.41	1.45	.07
37°C:						
Control	1,361	898	68	.25	1.93	.04
DBP deficiency:						
Type I (c.715_1261del)	47	2	5	2.07	2.66	.61
Type I (Q677X)	…	…	…	2.09	2.83	.76
Type II (N457D+I516T)	578	30	29	.56	1.75	.07
40°C:						
Control	854	680	35	.42	2.85	.09
DBP deficiency:						
Type I (c.715_1261del)	82	23	6	2.64	3.98	1.22
Type I (Q677X)	…	…	…	3.58	3.25	.97
Type II (N457D+I516T)	481	17	12	2.47	4.43	1.01

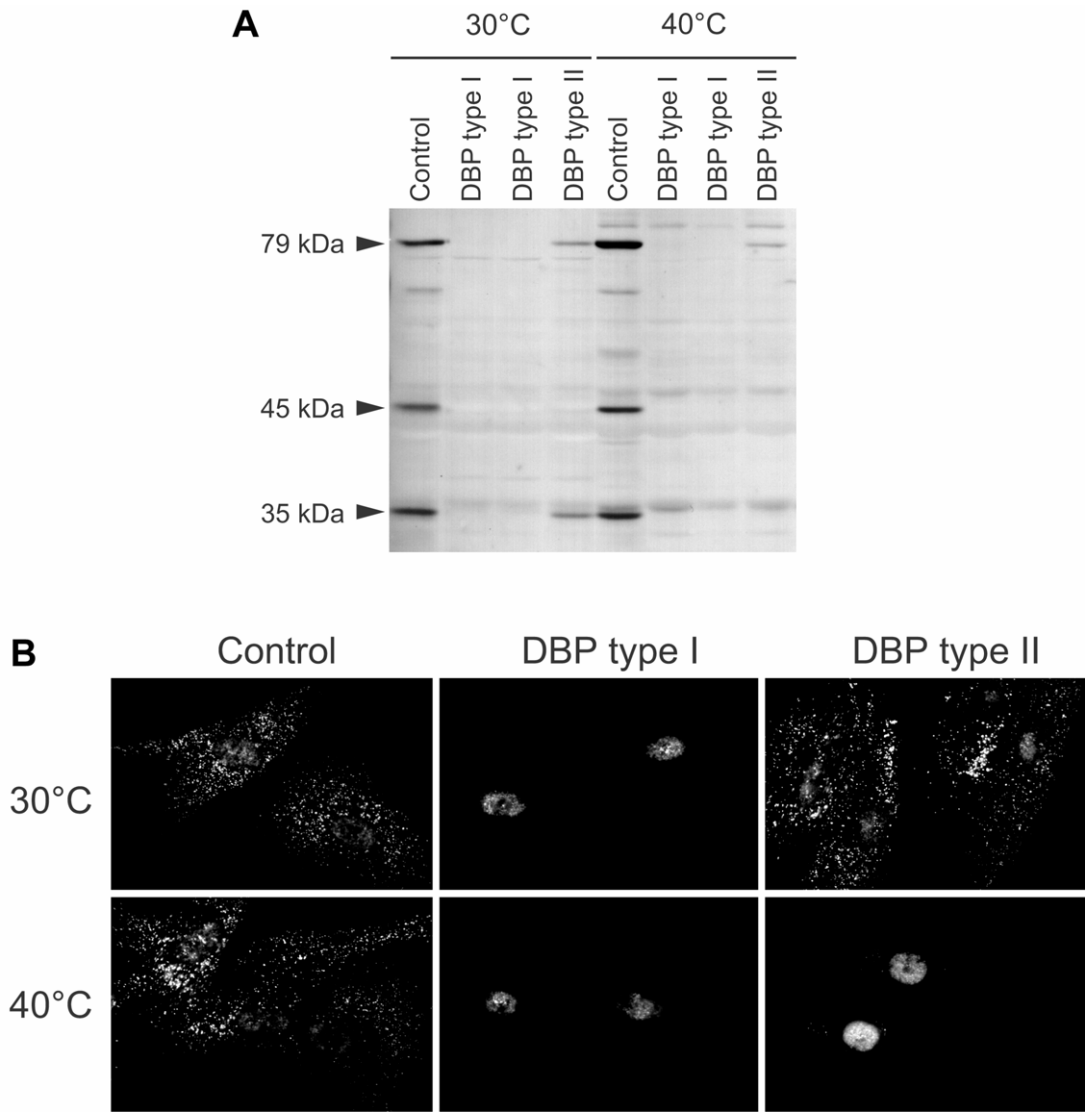

Figure 3 *A,* Immunoblot analysis with an antibody against human DBP in skin fibroblasts from one control subject, two DBP type I–deficient patients, and one patient with mild DBP type II deficiency that were cultured at 30°C and 40°C for 7 d. The arrowheads indicate the 79-kDa full-length protein, the 45-kDa enoyl-CoA hydratase plus sterol carrier protein 2–like units, and the 35-kDa 3-hydroxyacyl-CoA dehydrogenase unit. At 40°C, the 35-kDa band of DBP is absent in the fibroblasts of the patient with mild type II deficiency. *B,* DBP immunofluorescence microscopy in fibroblasts from a control subject, a DBP type I–deficient patient, and a patient with mild type II deficiency that were cultured at 30°C and 40°C for 7 d prior to immunofluorescence. At 30°C, the fibroblasts of the patient with mild type II deficiency show a normal punctate pattern of peroxisomes, like those of the control subject, whereas, at 40°C, the staining is negative.

of the different mutations on protein structure were studied using the available crystal structures. Cultured skin fibroblasts from all included patients were fully characterized at the biochemical level, and metabolite analysis in plasma, when available, was also been performed. In addition, for the majority of the patients, information about the age at death was available. The collected data provided us with the unique opportunity to study whether there is a correlation between genotype and phenotype in DBP deficiency, with the help of the protein structures of the different DBP domains.

The identified mutations caused a wide variety of changes in the structure of the DBP protein. Type I deficiency was always caused by gross defects of the DBP protein that were due to large deletions or truncations. The biochemical and clinical phenotype of type I–deficient patients is very severe, and all such patients die within the first 14 mo of life. The vast majority of type II– and type III–deficient patients have missense mutations in their *DBP* gene, and, for most of these patients, the biochemical and clinical presentation is also severe. Analysis of the protein structures *in silico* provided val-

uable information for studies of genotype-phenotype correlation. The disease-causing missense mutations were not randomly distributed along the DBP polypeptide. The effects of the missense mutations ranged from the replacement of catalytic residues or residues in direct contact with the substrate (mutations between amino acid residues 153–177 and 506–533 in the dehydrogenase and hydratase units, respectively) or the cofactor (mutations between amino acid residues 15–26) to disturbances of protein folding or dimerization of the subunits (mutations between amino acid residues 232–249). Only single mutations were found outside these hotspot regions.

Survival of >36 mo is rarely observed for patients with a DBP deficiency, and only these patients reach some psychomotor developmental milestones. In our cohort, there were eight patients who survived >36 mo. The results in this article that document the predicted structure of the mutated proteins of these patients with relatively mild presentations strongly suggest that the degree of deficiency of DBP activity contributes to the severity of the phenotype. Unfortunately, our DBP activity assay in cultured fibroblasts is not sensitive enough to measure subtle residual activities that are apparently very important for the outcome of the patients. Although environmental and genetic factors may influence phenotypic variation, it can be concluded, on the basis of the predicted effect of the mutations on protein structure, that a genotype-phenotype correlation exists for DBP deficiency.

Acknowledgments

We thank S. Denis, P. A. W. Mooyer, C. Dekker, J. Haasjes, and M. Malin, for technical assistance, and all the physicians who provided clinical data. This work was supported by the Dutch Organisation for Scientific Research (NWO) (grant 916.46.109), the Academy of Finland (grants 201262 and 211109 and, for research visits between the Research Council for Health of the Academy of Finland and NWO, grant 910.31.604), the Sigrid Jusélius Foundation, and the FP6 European Union Project "Peroxisomes" (LSHG-CT-2004-512018).

Web Resources

Accession numbers and URLs for data presented herein are as follows:

Online Mendelian Inheritance in Man (OMIM), http://www.ncbi.nlm.nih.gov/Omim/ (for DBP deficiency)

Protein Data Bank (PDB), http://www.rcsb.org (for entries 1GZ6, 1S9C, 1IKT, and 1ZBQ)

References

Adamski J, Carstensen J, Husen B, Kaufmann M, de Launoit Y, Leenders F, Markus M, Jungblut PW (1996) New 17 beta-hydroxysteroid dehydrogenases: molecular and cell biology of the type IV porcine and human enzymes. Ann N Y Acad Sci 784:124–136

Adamski J, Normand T, Leenders F, Monte D, Begue A, Stehelin D, Jungblut PW, de Launoit Y (1995) Molecular cloning of a novel widely expressed human 80 kDa 17 beta-hydroxysteroid dehydrogenase IV. Biochem J 311:437–443

Berman HM, Westbrook J, Feng Z, Gilliland G, Bhat TN, Weissig H, Shindyalov IN, Bourne PE (2000) The Protein Data Bank. Nucleic Acids Res 28:235–242

Bootsma AH, Overmars H, van Rooij A, van Lint AE, Wanders RJ, van Gennip AH, Vreken P (1999) Rapid analysis of conjugated bile acids in plasma using electrospray tandem mass spectrometry: application for selective screening of peroxisomal disorders. J Inherit Metab Dis 22:307–310

Dieuaide-Noubhani M, Asselberghs S, Mannaerts GP, Van Veldhoven PP (1997) Evidence that multifunctional protein 2, and not multifunctional protein 1, is involved in the peroxisomal beta-oxidation of pristanic acid. Biochem J 325:367–373

Ferdinandusse S, van Grunsven EG, Oostheim W, Denis S, Hogenhout EM, IJlst L, van Roermund CW, Waterham HR, Goldfischer S, Wanders RJ (2002) Reinvestigation of peroxisomal 3-ketoacyl-CoA thiolase deficiency: identification of the true defect at the level of D-bifunctional protein. Am J Hum Genet 70:1589–1593

Filling C, Berndt KD, Benach J, Knapp S, Prozorovski T, Nordling E, Ladenstein R, Jornvall H, Oppermann U (2002) Critical residues for structure and catalysis in short-chain dehydrogenases/reductases. J Biol Chem 277:25677–25684

Gloerich J, Denis S, Van Grunsven EG, Dacremont G, Wanders RJ, Ferdinandusse S (2003) A novel HPLC-based method to diagnose peroxisomal D-bifunctional protein enoyl-CoA hydratase deficiency. J Lipid Res 44:640–644

Guex N, Peitsch MC (1997) SWISS-MODEL and the Swiss-PdbViewer: an environment for comparative protein modeling. Electrophoresis 18:2714–2723

Haapalainen AM, Koski MK, Qin YM, Hiltunen JK, Glumoff T (2003) Binary structure of the two-domain (3*R*)-hydroxyacyl-CoA dehydrogenase from rat peroxisomal multifunctional enzyme type 2 at 2.38 Å resolution. Structure (Camb) 11:87–97

Haapalainen AM, van Aalten DM, Meriläinen G, Jalonen JE, Pirilä P, Wierenga RK, Hiltunen JK, Glumoff T (2001) Crystal structure of the liganded SCP-2-like domain of human peroxisomal multifunctional enzyme type 2 at 1.75 Å resolution. J Mol Biol 313:1127–1138

Itoh M, Suzuki Y, Akaboshi S, Zhang Z, Miyabara S, Takashima S (2000) Developmental and pathological expression of peroxisomal enzymes: their relationship of D-bifunctional protein deficiency and Zellweger syndrome. Brain Res 858:40–47

Jiang LL, Kobayashi A, Matsuura H, Fukushima H, Hashimoto T (1996) Purification and properties of human D-3-hydroxyacyl-CoA dehydratase: medium-chain enoyl-CoA hydratase is D-3-hydroxyacyl-CoA dehydratase. J Biochem (Tokyo) 120:624–632

Jiang LL, Kurosawa T, Sato M, Suzuki Y, Hashimoto T (1997*a*) Physiological role of D-3-hydroxyacyl-CoA dehydratase/D-3-hydroxyacyl-CoA dehydrogenase bifunctional protein. J Biochem (Tokyo) 121:506–513

Jiang LL, Miyazawa S, Souri M, Hashimoto T (1997*b*) Structure of D-3-hydroxyacyl-CoA dehydratase/D-3-hydroxyacyl-CoA dehydrogenase bifunctional protein. J Biochem (Tokyo) 121:364–369

Jones TA, Zou JY, Cowan SW, Kjeldgaard (1991) Improved methods for building protein models in electron density maps and the location of errors in these models. Acta Crystallogr A 47:110–119

Koski MK, Haapalainen AM, Hiltunen JK, Glumoff T (2004) A two-domain structure of one subunit explains unique features of eukaryotic hydratase 2. J Biol Chem 279:24666–24672

——— (2005) Crystal structure of 2-enoyl-CoA hydratase 2 from hu-

man peroxisomal multifunctional enzyme type 2. J Mol Biol 345: 1157–1169

Leenders F, Husen B, Thole HH, Adamski J (1994) The sequence of porcine 80 kDa 17 beta-estradiol dehydrogenase reveals similarities to the short chain alcohol dehydrogenase family, to actin binding motifs and to sterol carrier protein 2. Mol Cell Endocrinol 104: 127–131

Leesong M, Henderson BS, Gillig JR, Schwab JM, Smith JL (1996) Structure of a dehydratase-isomerase from the bacterial pathway for biosynthesis of unsaturated fatty acids: two catalytic activities in one active site. Structure 4:253–264

Malila LH, Siivari KM, Mäkelä MJ, Jalonen JE, Latipaä PM, Kunau WH, Hiltunen JK (1993) Enzymes converting D-3-hydroxyacyl-CoA to *trans*-2-enoyl-CoA: microsomal and peroxisomal isoenzymes in rat liver. J Biol Chem 268:21578–21585

Novikov D, Dieuaide-Noubhani M, Vermeesch JR, Fournier B, Mannaerts GP, Van Veldhoven PP (1997) The human peroxisomal multifunctional protein involved in bile acid synthesis: activity measurement, deficiency in Zellweger syndrome and chromosome mapping. Biochim Biophys Acta 1360:229–240

Paton BC, Pollard AN (2000) Molecular changes in the D-bifunctional protein cDNA sequence in Australasian patients belonging to the bifunctional protein complementation group. Cell Biochem Biophys 32:247–251

Paton BC, Sharp PC, Crane DI, Poulos A (1996) Oxidation of pristanic acid in fibroblasts and its application to the diagnosis of peroxisomal beta-oxidation defects. J Clin Invest 97:681–688

Paton BC, Solly PB, Nelson PV, Pollard AN, Sharp PC, Fietz MJ (2002) Molecular analysis of genomic DNA allows rapid, and accurate, prenatal diagnosis of peroxisomal D-bifunctional protein deficiency. Prenat Diagn 22:38–41

Qin YM, Haapalainen AM, Conry D, Cuebas DA, Hiltunen JK, Novikov DK (1997) Recombinant 2-enoyl-CoA hydratase derived from rat peroxisomal multifunctional enzyme 2: role of the hydratase reaction in bile acid synthesis. Biochem J 328:377–382

Qin YM, Haapalainen AM, Kilpeläinen SH, Marttila MS, Koski MK, Glumoff T, Novikov DK, Hiltunen JK (2000) Human peroxisomal multifunctional enzyme type 2: site-directed mutagenesis studies show the importance of two protic residues for 2-enoyl-CoA hydratase 2 activity. J Biol Chem 275:4965–4972

Qin YM, Marttila MS, Haapalainen AM, Siivari KM, Glumoff T, Hiltunen JK (1999) Yeast peroxisomal multifunctional enzyme: (3*R*)-hydroxyacyl-CoA dehydrogenase domains A and B are required for optimal growth on oleic acid. J Biol Chem 274:28619–28625

Schröder JM, Hackel V, Wanders RJ, Göhlich-Ratmann G, Voit T (2004) Optico-cochleo-dentate degeneration associated with severe peripheral neuropathy and caused by peroxisomal D-bifunctional protein deficiency. Acta Neuropathol (Berl) 108:154–167

Suzuki Y, Jiang LL, Souri M, Miyazawa S, Fukuda S, Zhang Z, Une M, Shimozawa N, Kondo N, Orii T, Hashimoto T (1997) D-3-hydroxyacyl-CoA dehydratase/D-3-hydroxyacyl-CoA dehydrogenase bifunctional protein deficiency: a newly identified peroxisomal disorder. Am J Hum Genet 61:1153–1162

van Grunsven EG, Mooijer PA, Aubourg P, Wanders RJ (1999*a*) Enoyl-CoA hydratase deficiency: identification of a new type of D-bifunctional protein deficiency. Hum Mol Genet 8:1509–1516

van Grunsven EG, van Berkel E, IJlst L, Vreken P, de Klerk JB, Adamski J, Lemonde H, Clayton PT, Cuebas DA, Wanders RJ (1998) Peroxisomal D-hydroxyacyl-CoA dehydrogenase deficiency: resolution of the enzyme defect and its molecular basis in bifunctional protein deficiency. Proc Natl Acad Sci USA 95:2128–2133

van Grunsven EG, van Berkel E, Mooijer PA, Watkins PA, Moser HW, Suzuki Y, Jiang LL, Hashimoto T, Hoefler G, Adamski J, Wanders RJ (1999*b*) Peroxisomal bifunctional protein deficiency revisited: resolution of its true enzymatic and molecular basis. Am J Hum Genet 64:99–107

Vreken P, van Lint AE, Bootsma AH, Overmars H, Wanders RJ, van Gennip AH (1998) Rapid stable isotope dilution analysis of very-long-chain fatty acids, pristanic acid and phytanic acid using gas chromatography-electron impact mass spectrometry. J Chromatogr B Biomed Sci Appl 713:281–287

Wanders RJ, Denis S, Ruiter JP, Schutgens RB, van Roermund CW, Jacobs BS (1995) Measurement of peroxisomal fatty acid beta-oxidation in cultured human skin fibroblasts. J Inherit Metab Dis 18:113–124

Wanders RJ, Van Roermund CW (1993) Studies on phytanic acid alpha-oxidation in rat liver and cultured human skin fibroblasts. Biochim Biophys Acta 1167:345–350

Wanders RJA, Barth PG, Heymans HSA (2001) Single peroxisomal enzyme deficiencies. In: Scriver CR, Beaudet AL, Sly WS, Valle D (eds) The molecular and metabolic bases of inherited disease. McGraw-Hill, New York, pp 3219–3256